JOURNAL OF CATALYSIS **176,** 235–245 (1998)
ARTICLE NO. CA982035

Role of the Support in Syngas Conversion over Pd/Cu–KL Zeolite Catalysts

James A. Anderson,*[,1] Manuel López-Granados,† and Marcos Fernández-García†

*Royal Society Research Fellow, Department of Chemistry, The University, Dundee DD1 4HN, Scotland, United Kingdom; and †Instituto de Catálisis y Petroleoquímica, CSIC, Cantoblanco, 28049-Madrid, Spain

Received October 29, 1997; revised January 12, 1998; accepted February 2, 1998

Infrared spectra are reported for a KL zeolite and copper and palladium-containing KL zeolites at high temperatures and under high pressures of CO/H_2 and the results discussed with reference to parallel reaction studies. Particular attention has been given to the role of the zeolite surface in the further conversion of methanol produced in the metallic function. The initial steps in the reaction are the formation of formyl type species from adsorbed H atoms and associatively adsorbed CO which generate methanol or spillover to produce adsorbed formate at potassium sites in the zeolite. These formate species undergo further reaction with adsorbed methanol to produce methyl formate. The formation of methyl formate from methanol contrasts with the established route for methanol to hydrocarbons over acidic zeolites where methanol is initially dehydrated to give dimethylether. This has been attributed to the failure to generate surface methoxy species on the basic zeolite. Acetate species located on the zeolite surface are produced from acetyl species on the metal surface followed by transfer to the support in the same manner as formate and are not generated via isomerisation of methyl formate. The alloying of Pd and Cu leads to enhanced hydrogenation behavior compared to the individual metals as reflected in the alkane/alkene ratios. © 1998 Academic Press

INTRODUCTION

The conversion of synthesis gas ($CO + H_2$) to higher value products such as methanol using the ICI $Cu/ZnO/Al_2O_3$ catalyst or into longer chain hydrocarbons via Fischer–Tropsch synthesis is well known and are well established processes. Methanol may be converted to hydrocarbons using ZSM-5 type catalysts which leads to a high proportion of iso-paraffins and benzene derivatives for use as a high octane gasoline. The direct conversion of synthesis gas to useful hydrocarbon fractions may be achieved by combining a methanol synthesis catalyst with a solid acid catalyst. For example, Fujimoto *et al.* (1) combined Pd/SiO_2 with H-ZSM-5 or H-Mordenite and obtained high selectivities to aromatic hydrocarbons, while Chang *et al.* (2) combined Zn–Cr mixed oxides with H-ZSM-5. It is generally believed that hydrocarbon formation proceeds initially via formation of dimethyl ether (DME) which is produced by reaction between methoxy groups bound to the acid catalyst surface and adsorbed methanol (3, 4). A hybrid catalyst composed of $Cu/ZnO/Al_2O_3$ and an ammonium treated zeolite has also been developed to produce DME in one step (5). While acid site containing zeolites favor the dehydration of methanol to give DME, dehydrogenation of alcohols is favored over silicalite and alkali metal cation-exchanged zeolites (6–8). Methanol dehydrogenation may lead to formation of methyl formate or formaldehyde (8) with the latter being the thermodynamically less favored under conditions normally used for CO hydrogenation.

Under high pressure gas phase conditions, methanol produced by CO hydrogenation may undergo further reaction with syngas mixtures to produce higher carboxylic acids (9). This may proceed either via CO insertion or by isomerisation of methyl formate (10).

In the current study, two metals, Cu and Pd, which are highly active and selective for methanol synthesis from syngas (11–13) have been combined with a basic zeolite (KL) in order to obtain further information regarding the mechanism and reaction scheme of secondary reaction products from CO/H_2 mixtures. The role of basic sites in the formation of hydrocarbons from methanol or higher alcohols has received much less attention than the corresponding reaction over acid sites (6). The surface and bulk characteristics of the metallic phases present in this series of catalysts have been studied under hydrogen alone and under CO/H_2 mixtures at elevated temperatures and pressures (14, 15). Reduction above 623 K produced a series of substitutionally disordered alloys with no detection of monometallic Cu or Pd phases. A synergetic effect on methanol production has been observed by alloying Pd and Cu, although the physical basis behind this enhanced activity has not been explained (16). IR studies of CO adsorption at room temperature indicate no significant segregation of copper within PdCu alloys (14), although under high pressure/high temperature conditions in the presence of CO and H_2, the surface becomes significantly enriched by Pd (15).

[1] Corresponding author.

0021-9517/98 $25.00

Catalytic testing of the above catalysts for CO hydrogenation indicates that there is a degree of activation of the samples during the first 24 h on-stream while previous IR studies indicate a progressive loss in threefold adsorption sites as a function of time in reaction during the same period (15). The present study was carried out with an objective to identify surface species present during the catalytic reaction and in particular to determine the role of the KL zeolite in the formation of products via methanol.

EXPERIMENTAL

Three bimetallic catalysts containing 1% Pd and 1, 0.5, and 0.25% Cu and two monometallic reference catalysts containing 1% Pd and 1% Cu were prepared by co-impregnating or impregnating KL-zeolite (Si/Al = 3.0 from Tosoh Corp., Japan) with the nitrate precursors, using NaOH solution to maintain the solution at pH 8. EPR analysis indicates that ca 0.01 wt% iron was present in both the fresh catalyst and in samples removed from the reactor. Sodium and potassium contents were calculated at 0.006 and 14.0 wt%. Samples were dried overnight at 373 K and then calcined at 573 K for 2 h in a flow of oxygen (0.4 l/min · g). XANES analysis of the samples reduced at 623 K detects a series of substitutionally disordered alloys with formal compositions $Pd_{33}Cu_{67}$, $Pd_{50}Cu_{50}$, and $Pd_{67}Cu_{33}$ with no evidence of monometallic Cu or Pd phases (14). XANES studies conducted under CO/H_2 at 573 K confirm that no disruption of these alloys occur in reaction (15).

Infrared Experiments

Samples in the form of pressed powder discs of 25 mm diameter were prepared by compacting the loose powder at 1.5 tons between two polished stainless steel dies. Catalyst discs were heated in a flow (100 cm^3 min^{-1}) of 3.5% H_2 in Ar at 5 K min^{-1} to 623 K before maintaining this temperature for 30 min. The cell was purged in a flow of dry nitrogen for 30 min at 623 K and cooled to 573 K. The sample was then outgassed in dynamic vacuum for 5 min at 573 K before introduction of the CO/H_2 mixture (1 : 2) at a total pressure of 10 bar. IR spectra were recorded at the reaction temperature as a function of reaction time using a Perkin Elmer 1720X Fourier transform spectrometer operating at a resolution of 4 cm^{-1} and accumulating 25 scans for each spectrum. Other experimental details including the use of the high pressure IR cell in CO hydrogenation are as previously reported (17, 18).

Infrared spectra of samples exposed to individual adsorbates were obtained using samples treated as for high pressure experiments except that, following reduction, dynamic vacuum was applied for 15 min at 623 K followed by transfer of the sample to the optical compartment of the IR cell where spectra were recorded at ambient temperature.

Catalytic Measurements

The catalytic tests were conducted in a tubular stainless steel reactor (10.5 mm ID). The sample (0.4 g) was calcined (573 K for 4 h in a N_2/O_2 mixture) in the reactor, reduced (100 cm^3 min^{-1} of 10 vol% H_2/He at 623 K for 1 h) and then exposed to the reaction mixture as a flow of 50 cm^3 min^{-1} H_2 and CO (CO/H_2 1 : 2, W/F = 0.122 g · h/l of $H_2 + CO$). Gas flows were controlled by electronic mass flow controllers and a K-type thermocouple buried in the catalytic bed, used to measure and control the temperature. Experiments were conducted between 493 and 553 K at 1 MPa overall pressure. Reactor effluent was analyzed by on-line GC (Hewlett-Packard 5730A) fitted with Poraplot Q and Molecular Sieve X5A columns. Outlet lines were heated at 423 K to prevent condensation of the reaction products. Product analysis was performed using a TCD detector for CO, CO_2, and H_2O and FID for C_1–C_9 hydrocarbons, C_1–C_4 alcohols, ethers, esters, and acids. Blank experiments conducted under the above reaction conditions using silica or alumina produced no detectable products.

TPD Measurements

100 mg of sample were placed in a stainless steel reactor connected to a vacuum line and gas handling system. These were calcined and reduced following the procedure for catalytic testing and subsequently treated in He at 623 K for 30 min before cooling to 298 K. Two types of experiments were performed using these preconditioned samples. The first was aimed at determining the importance of C–O dissociation paths in which after treatment in CO at 523 K for 30 min and cleaning the surface at the same temperature with He, a TPR in 0.5% H_2/He was performed raising the temperature at 5 K min^{-1} from room temperature to 623 K. The second set of experiments was carried out to determine the possible role of methyl formate as an intermediate in hydrocarbon production. Two percent H_2/He was bubbled through a saturator filled with methyl formate (MF) maintained at 193 K (ca 0.5% MF) and passed over the catalyst while heating at 5 K min^{-1} from room temperature to 623 K. This experiment was also performed using a 2% H_2–1% CO/He mixture. Desorbed products were analyzed by a quadrupole mass filter (BALZERS QMG 125) connected to the reactor outlet.

RESULTS

Selectivities for CO hydrogenation at temperatures required to obtain ca 2% CO conversion are shown in Table 1. The KL zeolite alone shows activity for hydrocarbon and methanol formation, although significant activity with a C-distribution (i.e., a maximum in selectivity at C_4) and oxygenate selectivity typical of the metal-loaded samples are only obtained when methanol is added to the feed.

TABLE 1

Selectivities at 2% CO Conversion

	KL	KL(+CH_3OH)	Pd–KL	Cu–KL	PdCu(0.25)	PdCu(0.5)	PdCu(1.0)
Temperature/K	526	513	508	505	504	506	506
Yield (C wt%)							
Hydrocarbons	81.7	92.1	92.7	67.8	91.1	90.1	93.7
Oxygenates	16.7	4.9	7.4	9.3	8.9	9.9	6.3
CO_2	2.6	3.0	0.0	22.9	0.0	0.0	0.0
Hydrocarbon distribution (C at%)							
C_1	23.4	19.8	20.0	16.8	17.7	13.8	16.1
C_2	19.9	15.2	12.1	8.3	10.8	12.0	11.7
C_3	16.1	16.9	14.6	9.0	13.6	14.6	14.9
C_4	12.7	17.4	16.0	10.5	15.3	16.6	15.7
C_5	5.7	11.2	12.5	6.9	10.2	10.6	10.8
C_6	2.8	7.5	7.8	6.5	9.6	9.1	8.9
C_7	1.1	7.1	6.1	5.3	8.9	8.8	7.6
C_8	0.0	2.1	3.6	3.3	4.9	4.5	4.8
C_9	0.0	0.0	0.0	1.2	0.0	0.0	3.7
Oxygenate distribution (C at%)							
CH_3OH	61.4	49.0	45.3	49.3	43.2	47.6	59.5
C_2H_5OH	33.0	51.0	54.7	51.7	56.8	52.4	35.5
C_3H_7OH	5.4	0.0	0.0	0.0	0.0	0.0	5.0

At low levels of conversion, no CO_2 is observed for any of the Pd containing samples.

Figure 1 displays activities in terms of CO conversion for two reaction temperatures as a function of copper content of the various samples. The two plots indicate that maximum activity corresponds with PdCu(0.25)/KL. Leon y Leon and Vannice (16) observed similar maxima for CO hydrogenation over $PdCu/SiO_2$ in plots of methanol and methane TOF although the maxima corresponded with a composition of 59 as opposed to 0.295 at% copper as indicated in Fig. 1. However, differences between these results may be expected given that the silica-supported sample contained unalloyed copper in addition to the bimetallic particles, whereas only bimetallic particles were present in the case of the KL support (14). Selectivity in terms of paraffin to olefin ratio as a function of CO conversion is shown in Fig. 2. Increased levels of conversion lead to enhanced P/O

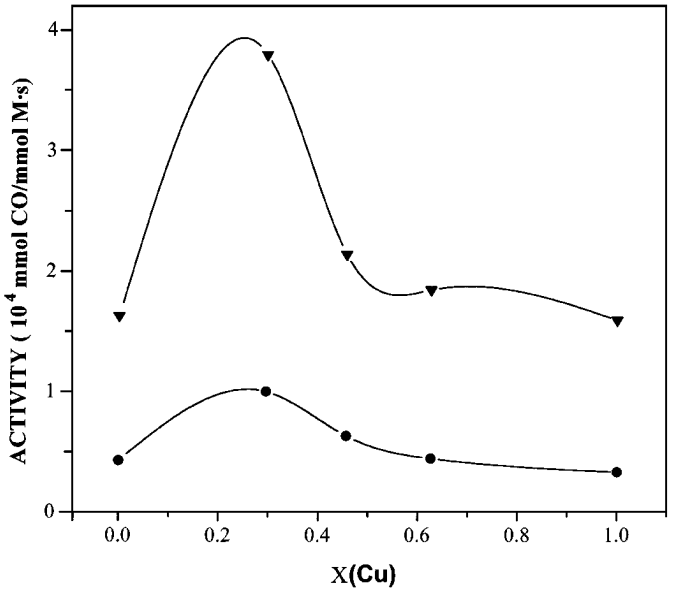

FIG. 1. Influence of copper content on the CO conversion activity of PdCu/KL catalysts in CO/H_2 (1 : 2), 1 MPa total pressure and reaction temperatures of 493 (●) and 533 K (▼).

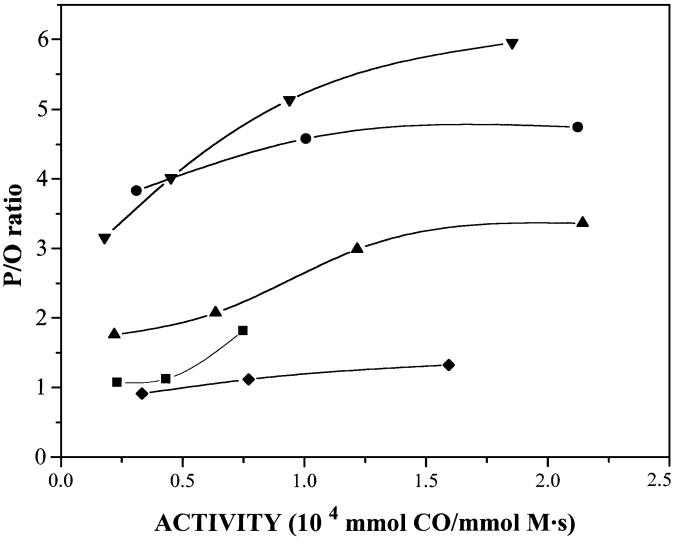

FIG. 2. Ratio of paraffins to olefins as a function of catalyst activity for (◆) Cu/KL, (■) Pd/KL, (●) PdCu(0.25)/KL, (▲) PdCu(0.5)/KL, and (▼) PdCu(1.0)/KL in CO/H_2 (1 : 2), 1 MPa total pressure, W/F = 0.122 g · h/l in the temperature range 493–553 K.

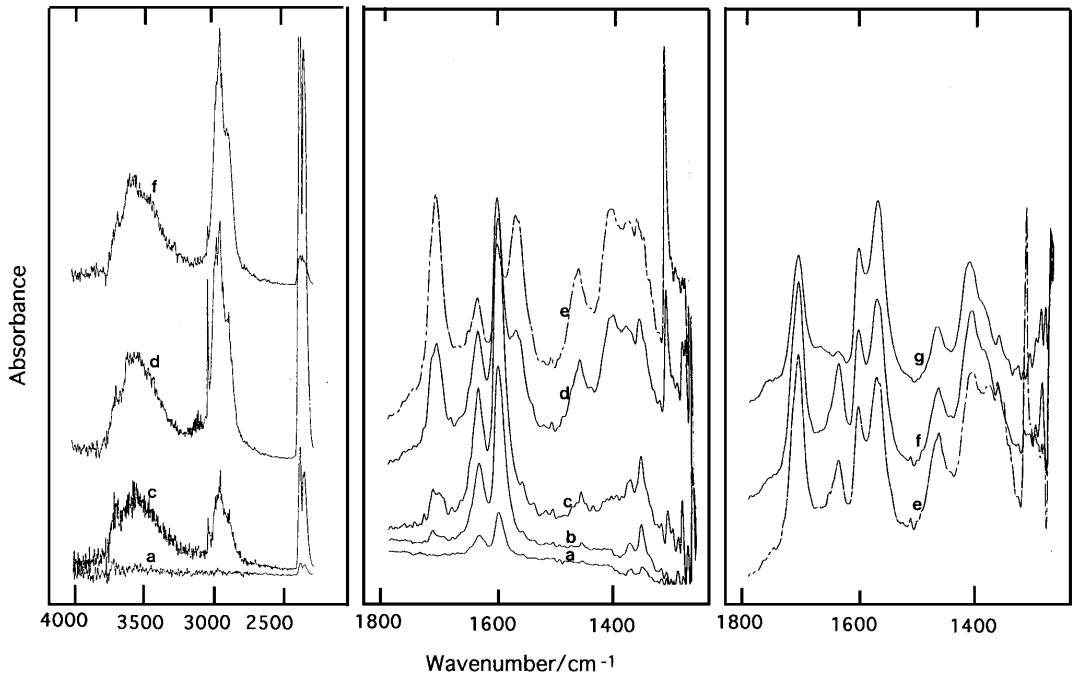

FIG. 3. IR spectra of KL zeolite reduced at 623 K and exposed to CO/H_2 (1 : 2) at 1 MPa total pressure at 573 K for (a) 1, (b) 10, (c) 60 min, (d) 5 and (e) 19 h, then (f) pressure released to 0.1 MPa, (g) evacuation at 573 K for 1 min.

ratios indicating that some if not all paraffins were formed via hydrogenation of the corresponding olefin. The alloying of palladium and copper enhanced hydrogenation activity with respect to the individual metals.

In Fig. 3, selected spectra are displayed of the KL zeolite in CO/H_2 at 573 K as a function of time. Spectra show a progressive increase in intensity of bands at ca 3650, 3500, 3015, 2966, 2933, and 2886 cm^{-1}. Bands in the 2300–2400 cm^{-1} region can be assigned to gaseous CO_2 generated in the IR cell as indicated by the steady increase in intensity as a function of the reaction time and the abrupt decrease following release of the pressure in the cell to 0.1 MPa (Fig. 3f). These bands were absent following brief evacuation at 573 K. The band at 3015 cm^{-1} was similarly affected by changes to the total pressure and can be assigned to gaseous CH_4 (17).

After 1 min had elapsed, the spectrum showed adsorbed water (1635 cm^{-1}) and formate species (1598, 1371, and 1351 cm^{-1}) and possibly a very weak band at 1453 cm^{-1} (Fig. 3a). The latter was confirmed by a progressive growth at this frequency as a function of reaction time. Further periods in reaction also lead to the identification of a band at 1305 cm^{-1} due to gaseous methane (17) and a doublet at 1717/1706 cm^{-1}. As a function of time, the latter became the dominant feature until, after extended periods, only the lower frequency maximum was recognised (Fig. 3e). A band at 1567 cm^{-1} due to the ν_a(OCO) of acetate species, was initially much less intense than the 1598 cm^{-1} formate band but after extended periods in reaction became the dominant of the two (Fig. 3e). The band due to adsorbed water was reduced in intensity while the pair at 1371 and 1351 cm^{-1} was accompanied by a third band of equivalent intensity at 1400 cm^{-1}. Of this triplet, only the latter retained its full intensity after releasing the pressure within the cell, a procedure which led to a decrease in the band due to gaseous CH_4 and an increased intensity at 1635 cm^{-1}, indicating further formation of water (Fig. 3f). Most of this was removed by brief evacuation at 573 K (Fig. 3g).

Figure 4 compares the spectra obtained for all catalysts after exposure to the CO/H_2 mixture for 19 h. All of the spectral features observed are as reported for the zeolite alone as a function of time (Fig. 3) with the appearance/nonappearance and different relative intensities of the various IR bands reflecting the relative degrees of conversion within the IR cell. The spectra for the three bimetallic catalysts after 19 h were almost identical, both in terms of the presence and intensities of the bands (Figs. 4d, e, f). The two monometallic catalysts appear to have reached lower levels of conversion to products as judged by the low intensities of bands at 3015 and 1305 cm^{-1} and the rotational fine structure between 3200–3020 cm^{-1} due to gaseous methane, the low band intensities due to adsorbed hydrocarbons between 3000–2800 cm^{-1} and in the range 1500–1300 cm^{-1}, and the absence of the ca 1710 cm^{-1} maximum observed for other samples (Figs. 4a, b). The exception to the above was the band at 1598 cm^{-1} due to adsorbed formate which was of greater intensity than for any of the bimetallic samples or the zeolite alone after a similar length of time in reaction.

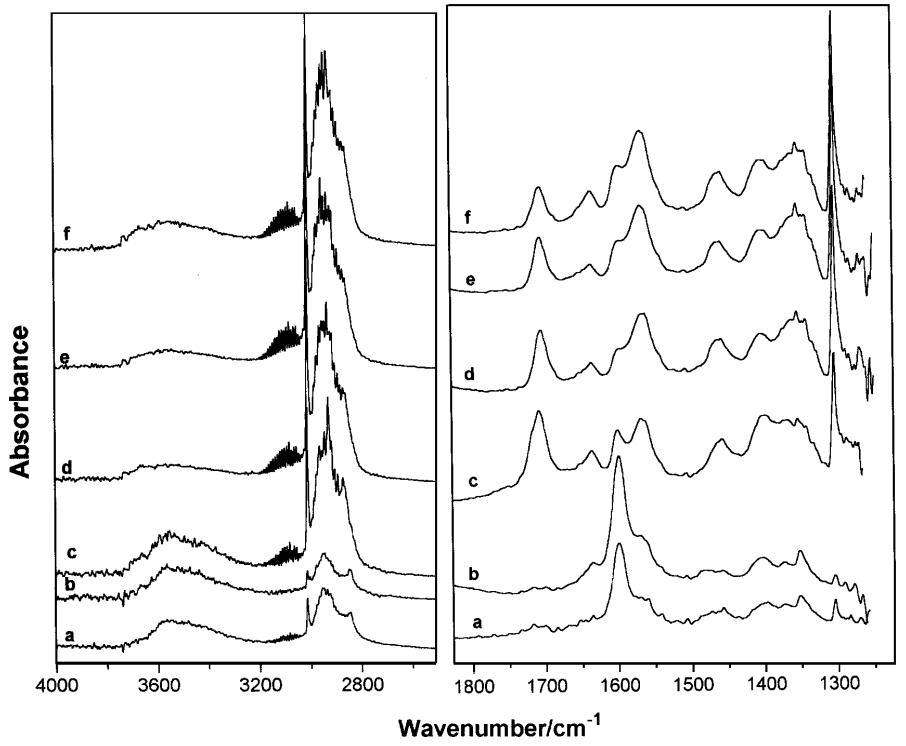

FIG. 4. Spectra of samples recorded 19 h after exposure to CO/H_2 (1:2) at 1 MPa total pressure and 573 K: (a) Cu/KL; (b) Pd/KL; (c) KL; (d) PdCu(0.25)/KL; (e) PdCu(0.5)/KL; (f) PdCu(1.0)/KL.

However, this is consistent with the observation for KL as a function of time (Fig. 3), where formate dominates at short reaction times but is depleted after extended periods while growth in the surface acetate concentration continues. Although the spectrum of Cu/KL shows a greater level of adsorbed hydrocarbons than Pd/KL, the former in contrast to the behavior of Pd/KL, showed no evidence for the formation of adsorbed water throughout the duration of the experiment.

The evolution of species responsible for bands at ca 1710, 1598, and 1567 cm^{-1} was followed by plotting band intensities as a function of time for the reduced KL zeolite (Fig. 5A) and PdCu(0.5)/KL as an example of a supported bimetallic catalyst (Fig. 5B). Plots show an initial

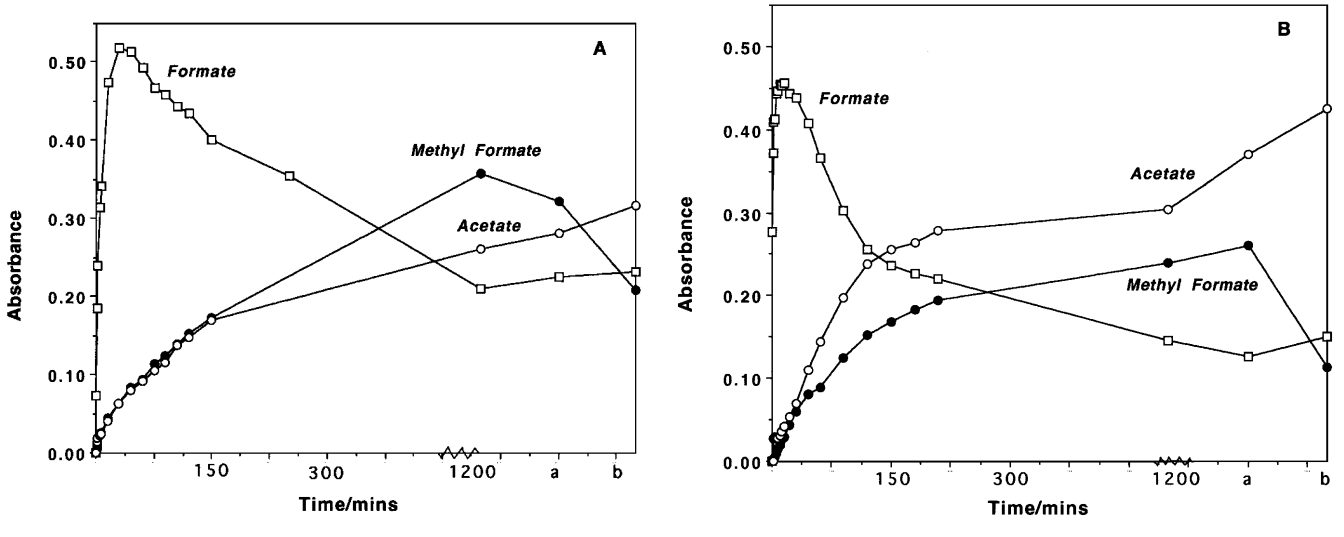

FIG. 5. Evolution of IR bands at 1710 (●), 1598 (□), and 1567 cm^{-1} (○) as a function of reaction time in CO/H_2 (1:2) at 1 MPa total pressure at 573 K for (A) KL zeolite and (B) PdCu(0.5)/KL, followed by (a) release of pressure to 0.1 MPa and (b) brief evacuation at 573 K.

rapid growth in formate concentration (1598 cm^{-1}) reaching a maximum concentration after 30 min for the PdCu example and after 60 min for the zeolite alone, followed by a decrease in surface concentrations. Bands at 1710 and 1567 cm^{-1} developed at an equivalent rate over the KL sample. For reaction times up to 300 min, the evolution of the species giving the band at 1710 cm^{-1} was identical for the PdCu/KL sample as for the zeolite alone whereas the rate of increase in surface acetate concentration (1567 cm^{-1}) exceeded that observed for the zeolite alone. The concentration of species giving the latter band was the most affected by brief evacuation at 573 K.

To assist in the assignation of bands in determining the role of the zeolite in the conversion of primary products into adsorbed species and secondary products, the adsorption of methanol, methyl formate, carbon dioxide, and carbon monoxide were studied. Additionally, the adsorption of pyridine was studied in order to confirm or negate the possible role of Brønsted acidity in the formation of products.

The zeolite in the absence of adsorbates showed two bands in the OH stretching region at 3741 and ca 3690 cm^{-1} (Fig. 6a). Exposure to low vapor pressures of methanol did not appear to influence these hydroxyl species, but led to the appearance of a broad maximum at ca 3500 cm^{-1} (3550/3420 cm^{-1}) and four defined bands in the CH stretching region at 2986, 2954, 2932, and 2842 cm^{-1} (Fig. 6b). Increasing the total pressure, followed by brief evacuation, led to the slight depletion of surface hydroxyl species, enhanced intensities at 3500 cm^{-1}, and of the bands due to CH stretching modes (Fig. 6c). In the lower frequency region, bands at 1480, 1464, 1453, and 1387 cm^{-1} due to CH deformation modes and a band at 1634 cm^{-1} became more pronounced with the latter inferring the presence of molecular water. An additional feature was a weak band at 2010 cm^{-1}, indicating adsorbed carbon monoxide. This is not due to adsorption on the zeolite itself (11) and indicates the presence of traces of reduced metal. The formation of carbonyl species infers some decomposition of methanol at 298 K. Heating the zeolite in the presence of methanol vapor at the temperature of the CO hydrogenation reaction, followed by evacuation on cooling to prevent readsorption of methanol vapor on the sample, led to a spectrum showing reduced intensities of all features with no indication for the formation of additional adsorbed species.

Adsorption of pyridine at room temperature on a sample of KL reduced at 623 K in either the presence of pyridine vapor or after evacuation at 413 K allowed bands at 1440, 1489, 1570, 1584, 1590, and 1603 cm^{-1} to be identified. All of these may be assigned to coordinatively bound or physisorbed pyridine with no evidence for Brønsted acidity.

A reduced sample of KL zeolite in the presence of CO at ambient temperature displayed only very weak bands at 2158 and 2118 cm^{-1} and a band at 1635 cm^{-1} due to adsorbed water contamination (Fig. 7a). The first pair corresponds with bands observed for CO adsorption on

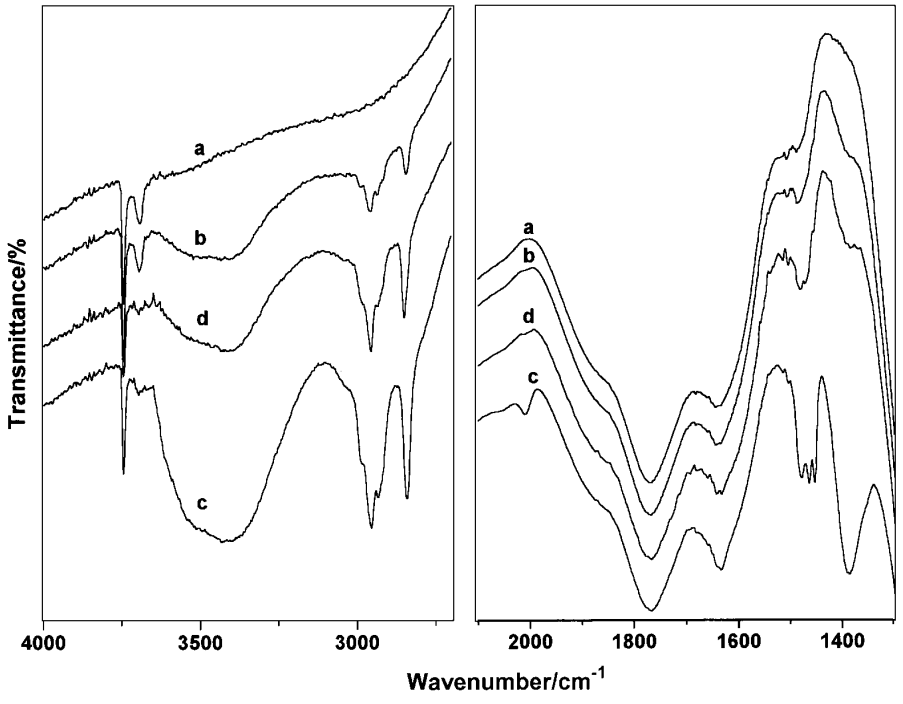

FIG. 6. Spectra of (a) KL zeolite reduced at 623 K; then (b) exposed to CH_3OH vapour at 298 K, pressure less than 13.3 Pa; (c) pressure less than 133 Pa, followed by evacuation at 298 K; (d) heated in 267 Pa CH_3OH vapour at 573 K (15 min) and evacuation at 298 K.

metal-loaded zeolites and is assigned to CO adsorption on the zeolite (14). Following heating in the presence of CO, weak, broad bands appeared at ca 1680 and 1355 cm^{-1}, in addition to the increased intensity of the band due to adsorbed water. CO_2 adsorption at 298 K led to the appearance of a similar band pair at ca 1680/1355 cm^{-1} as observed for CO, in addition to features at 1560, 1381, and 1270 cm^{-1} (Fig. 7d). Sharp bands appearing at 2394, 2339, and 2280 cm^{-1} (not shown) may all be attributed to physically adsorbed forms of CO_2. Heating in CO_2 at 573 K led to enhanced band intensities in the 1700–1300 cm^{-1} region, particularly of the 1680 cm^{-1} band, and to the appearance of a maximum at 1635 cm^{-1} due to adsorbed water (Figs. 7e, f).

The adsorption of methyl formate on a reduced sample of KL zeolite resulted in the appearance of IR bands at 2959, 1728, 1714, 1633, 1453, and 1435 cm^{-1} (Fig. 8a). At this level of surface coverage, no perturbation of hydroxyl species was observed, although at a coverage equivalent to that giving the spectrum in Fig. 8b, the lower frequency hydroxyl at ca 3690 cm^{-1} was perturbed and two broad maxima at 3425 and 3245 cm^{-1} were observed. This higher coverage also allowed additional maxima at 3041, 3015, 2870, and 2844 cm^{-1} to be discerned in addition to the previously noted 2959 cm^{-1} band. An increase in all previously mentioned maxima in the 1800–1250 cm^{-1} range (Fig. 8b) was observed and additional weak features at ca 1600 and 1383 cm^{-1} became apparent. Heating the sample at 573 K led to an increase in pressure within the IR cell consistent with the decomposition of methyl formate. The 1600 and 1383 cm^{-1} features were considerably enhanced following this brief period of heating followed by cooling in the presence of the vapor allowing methyl formate to readsorb on the surface (Fig. 8c). This procedure was repeated but this time evacuating during cooling to prevent readsorption, thus allowing bands due to this product to be distinguished from those due to the adsorbed methyl formate. Maxima were observed at 2957, 2849, 1598, 1371, and 1351 cm^{-1} in addition to weak bands due to residual methyl formate.

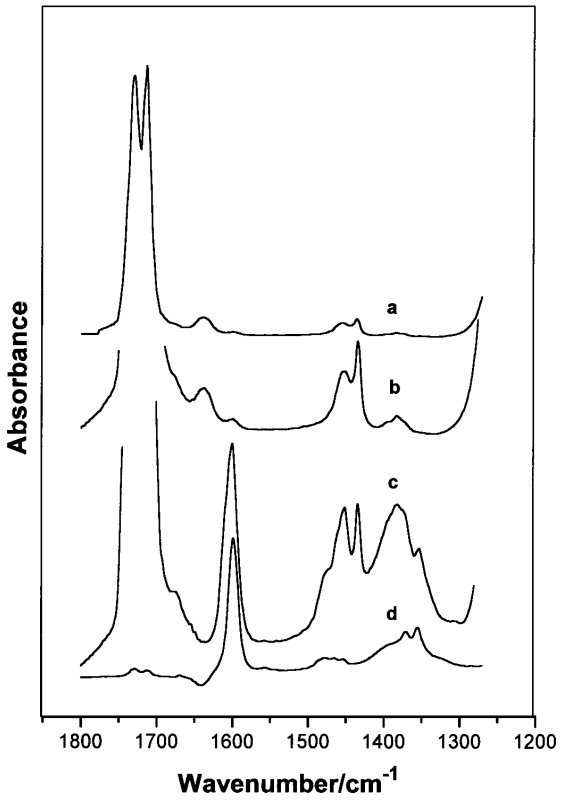

FIG. 8. IR spectra recorded at 298 K of KL zeolite reduced at 623 K and exposed to methyl formate (a) at 298 K, pressure ≪13.3 Pa; (b) at 298 K, pressure <13.3 Pa, (c) heating at 573 K (10 min) and cooling to 298 K in methyl formate; (d) heating at 573 K (1 h) followed by cooling to 298 K in dynamic vacuum.

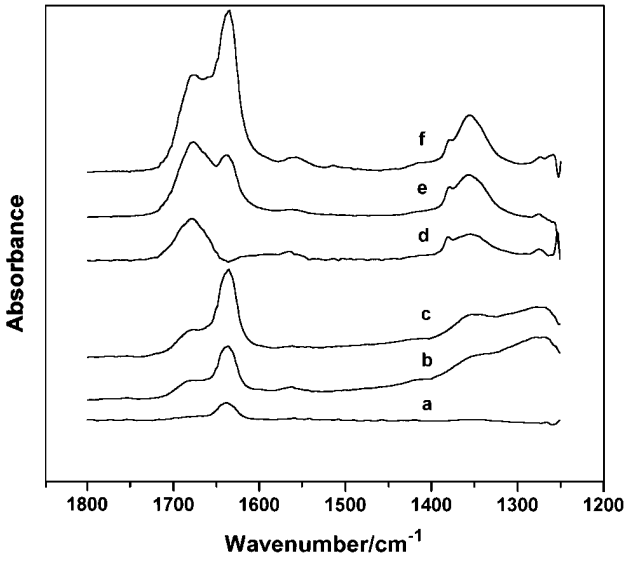

FIG. 7. IR spectra recorded at 298 K of KL zeolite reduced at 623 K and exposed to 1.33 kPa of CO (a) at 298 K, (b) 573 K for 1 h, and (c) 573 K for 19 h. Similarly pretreated KL zeolite exposed to 1.33 kPa CO_2 (d) at 298 K, (e) 573 K for 1 h, and (f) 573 K for 19 h.

MS analysis of products evolved during a TPR run from room temperature following CO adsorption at 523 K did not yield hydrocarbons which would implicate CO dissociation. Trace quantities of water above 373 K was the only product detected. Temperature programmed treatments of catalysts in the presence of hydrogen and methyl formate (plus CO in an additional experiment) generated only $H_2 + CO$ above 473 K and small amounts of CO_2 above 573 K.

DISCUSSION

Surface Hydroxyls and Acidity

Infrared spectra of the reduced K form L zeolite indicate at least two types of hydroxyl species (Fig. 6a) with stretching frequencies of 3741 and ca 3690 cm^{-1}, with the

latter sometimes resolved to give two maxima at 3699 and 3672 cm^{-1}. The 3741 cm^{-1} band is observed in other zeolite types, layer silicates, and amorphous silica (19–22) and may be assigned to silanol groups terminating the zeolite lattice at the external surface (21, 22). Spectra of KL may (20) or may not show IR bands due to structural hydroxyls (20, 23) after thermal treatment. Bands at 3700 and 3685 cm^{-1} have been assigned to residual water bound to potassium cations in KL (20). In a recent study (23), a band at 3674 cm^{-1} was observed following adsorption of water on Pt/KL and ascribed to the OH stretching mode of the free H atom in a water molecule simultaneously bound to Si–O–Al and K^+. The omnipresence of a band at 1635 cm^{-1} (Figs. 6–8) due to the OH deformation of adsorbed water helps confirm this assignment to K^+ bound water rather than to structural OH groups. Of significance in this study is the absence of a band at ca 3650 cm^{-1} (23) due to Brønsted acidic hydroxyls on the L zeolite.

Confirmtion of the absence of Brønsted acidity on KL was provided by the adsorption of pyridine which failed to detect absorption bands of the pyridinium ion. This would suggest either the absence of sites of suitable acid strength to protonate pyridine, or their location in areas inaccessible to the adsorbate. The latter is consistent with the conclusions (24) that any Brønsted acidity in BaK-L samples was located in the locked cages and as such did not participate in acid reactions. Metal-loaded samples have been prepared by impregnation at basic pH rather than ion exchange, thus avoiding the development of Brønsted acidity on reduction. The similarity between product selectivities for metal-loaded and metal-free KL zeolite and the similarity in the formation of adsorbed species detected by IR (Fig. 4) would confirm that no additional acidity was created by the incorporation of the metallic function and that any role of Brønsted acidity in the reaction mechanism can be discarded.

Methanol Adsorption

The absence of accessible protons within the zeolite matrix should exclude the assignment of absorption bands resulting from adsorption of methanol (Fig. 6) to vibrations of the methoxonium ion. The detection of $CH_3OH_2^+$ using IR spectroscopy (25) has been questioned since the species either rapidly eliminate water to form methoxy groups (23) or exist as a transient state rather than as an adsorbed intermediate (26). The absence of Evans window features (27) would indicate that methanol is not strongly hydrogen bonded to the KL zeolite. The 3550/3420 cm^{-1} absorption doublet detected at low methanol coverage but negligible depletion of either the high or low hydroxyl band (Fig. 6b) indicates that the initial adsorption mode does not involve the formation of methoxy species via condensation reaction with surface hydroxyls but reflects the perturbation of the methanol OH bond leading to two types of adsorption modes. The shift in the methanol OH on adsorption is somewhat greater than the ca 75 cm^{-1} shift observed for adsorption on Na^+ cations in NaZSM5 (22, 28). No OH vibrations were observed for methanol adsorption on either K^+/SiO_2, $Cu/K^+/SiO_2$, or $Pd/K^+/SiO_2$ (29, 30). In addition to interactions of the methanol OH with K^+ cations, the OH may interact through the H with Si–O–Al groups, explaining the presence of the doublet in the OH region (Fig. 4). Higher methanol coverage or heat treatment at 573 K did lead to loss in intensity of zeolite hydroxyls but no additional bands were observed due to CH stretching modes (Figs. 5c, d), suggesting perturbation of the low frequency zeolite hydroxyl rather than consumption during the formation of surface methoxy species. The absence of reaction with SiOH groups to form SiOMe contrasts with methanol adsorption on SiO_2 (17, 19), K^+/SiO_2 (26, 27), M/SiO_2 (where M = Rh, Cu, Pd) catalysts (17, 29, 30), $K^+/M/SiO_2$ (29, 30), and H-ZSM5 (22). No additional adsorbed species were generated by heat treatment at 573 K (Fig. 4d), indicating that the formate species (bands at 1598, 1371, and 1351 cm^{-1}) observed under CO/H_2 (Figs. 3, 4) is not derived by oxidation of methanol. This contrasts with Al_2O_3, MgO, and ZrO_2 (33–35), where methoxide species generated from methanol adsorption may be oxidised to formate species in the presence of the alcohol.

CO/CO_2 Adsorption

CO or CO_2 adsorption in the absence of hydrogen failed to generate formate species (Fig. 7) unlike ZrO_2, Al_2O_3, and MgO (35, 36), where formate may be generated by the reaction of CO with hydroxyl groups at temperatures below 573 K. As the reaction may proceed via an acylium cation (36), the absence of Brønsted acidic hydroxyls in the KL structure would account for this. Formate species observed under reaction conditions (Figs. 3, 4) are generated either by direct reaction between adsorbed CO and adsorbed hydrogen atoms or via adsorbed formyl species (13, 37).

Methyl Formate Adsorption

Results for methyl formate adsorption at 298 K (Fig. 8) are consistent with reports for adsorption on other oxides (10, 38) and K^+/SiO_2, Cu/SiO_2, and $Cu/K^+/SiO_2$ (29, 39). At 298 K, a transformation occurred which could be enhanced by heat treatment and resulted in the appearance of IR bands at 1598, 1371, and 1351 cm^{-1} due to adsorbed formate species (10, 29, 38). Decomposition of methyl formate should also generate adsorbed methoxy or methanol species. The enhanced intensities at 1453, 1435, and 1383 cm^{-1} on cooling in the closed system (Fig. 8c) confirm this and are consistent with results for methanol adsorption (Fig. 6). Evacuation removed unreacted methyl formate and other adsorbed species, indicating that methanol, rather than a surface bound methoxy species had been generated. Unlike rare earth oxides (10),

no acetic acid or acetate species were formed by isomerisation of methyl formate (40).

Overall Reaction Scheme

Water (1635 cm^{-1}) was detected during the initial stages of reaction over KL (Fig. 3a) but not for Cu/KL, even after extended periods of reaction (Fig. 4a). The high selectivity to CO_2 for CuKL at low conversions, unlike all other samples (Table 1), would suggest that any water present was converted by reaction with CO via the water–gas shift (wgs) reaction over this catalyst. Traces of water were always present in the zeolite, even after evacuation procedures at elevated temperatures (Fig. 7a) Surface formate species may (41, 42) or may not (43) act as an intermediate in the wgs reaction over solid acid and copper-based catalysts.

CO or CO_2 in the absence of hydrogen failed to generate formate, suggesting that the species produced during the initial stages of the reaction (Fig. 3a) is formed by the interaction of adsorbed CO and adsorbed hydrogen, the latter being generated by the metal component of the catalyst (reduced metal impurities, e.g. Fe in the case of the KL zeolite alone). This was confirmed by comparing the rates of formation of formate for the supported metal samples and the support alone (Fig. 5). Although the hydrogen required is generated on the metal surface, the formate species detected by bands at 1598, 1371, and 1351 cm^{-1} are not located on the metal, but are produced by either spillover hydrogen atoms or formyl species (13, 36). The frequencies agree with those attributed to unidentate formate for K^+/SiO_2 samples (29). A similar unidentate formate species was generated by decomposition of methyl formate (Fig. 8) which also led to the formation of adsorbed methanol rather than surface-bound methoxy groups (10, 29). Bands at 1717/1706 cm^{-1} detected for the CO/H_2 reaction can be partly attributed to methyl formate produced as the reverse of the decomposition reaction shown in Fig. 8. An alternative assignation of these bands would be to adsorbed formaldehyde (39) which is produced by dehydrogenation of methanol over acid-free crystalline silicates (7, 8). However, below 720 K, dehydrogenation to give formaldehyde is not thermodynamically favored (8) and no band at ca 1502 cm^{-1} (39) due to the CH_2 bending mode of this molecule was detected. While this may be due to the rapid conversion to polymeric formaldehyde species which is facilitated in the presence of potassium (39), the absence of characteristic bands at 1483, 1426, and 1392 cm^{-1} due to CH deformation modes of trioxane and polyoxymethylene (39) would confirm that methyl formate rather than formaldehyde is the species formed.

The above reaction sequence requires the formation of methanol prior to methyl formate. Methanol is produced predominantly on the metallic function but undergoes further transformation within the zeolite channels as indicated in the second column of Table 1, where cofeeding methanol over KL shifts the selectivities towards those obtained for the metal loaded KL. Results from Table 1 and Fig. 1 indicate that Pd-rich alloys approaching 30 at% copper appear to produce the maximum yield of methanol. As the surface concentration of copper in the substitutionally disordered FCC alloys is substantially depleted under reaction conditions (15), a beneficial geometrical arrangement with formation of binary centres must be ruled out and an electronic influence of subsurface copper may be postulated to interpret the catalytic behaviour of the samples. Significant electronic effects of Cu on Pd upon alloying have been reported recently (44). The presence of methanol desorbed from the metallic function within the zeolite prior to methyl formate generation can be deduced from the IR results. Figure 3a reveals a band at 1453 cm^{-1} in the absence of the carbonyl stretching mode of methyl formate at 1717/1706 cm^{-1}. Although the CH deformation mode of the methyl group of both methanol and methyl formate give rise to a band at 1453 cm^{-1} (Figs. 6, 8), the greater absorption coefficient of the carbonyl stretching mode of methyl formate to the methyl deformation would mean that the former would be the more readily detected at low concentrations. Similarly, throughout the reaction the relative intensities of bands at 1717/1706 and 1453 cm^{-1} are much closer than they appear in the spectrum of adsorbed methyl formate alone (Fig. 8a) and so the latter can be assumed to contain contributions from methyl groups of both methanol and methyl formate. However, the initial detection of the band in the absence of the 1717/1706 cm^{-1} pair signifies the formation of methanol prior to methyl formate.

The reaction between methanol and the adsorbed unidentate formate to produce methyl formate proceeds in the absence of the metal function. This is confirmed in Fig. 5, where the rate of formation of methyl formate is identical for PdCu/KL and the zeolite alone. Methyl formate was produced industrially by the reaction of CO and methanol over sodium hydroxide and it is known that alkali–metal promoted copper systems lead to enhanced methyl formate production (39). As sodium is absent in the case of KL alone, and the bands detected at 1598, 1371, and 1351 cm^{-1} are consistent with those due to formate on potassium in K^+/SiO_2 samples (29), it may be concluded that formate is generated at potassium sites in the zeolite, where it undergoes further reaction with methanol to generate methyl formate.

Chateau *et al.* (10) believe that two mechanisms are involved in the formation of carboxylic acids from methanol and syngas over rhodium catalysts. The first involves CO insertion on the rhodium component while the other proceeds via isomerisation of methyl formate on the support. The absence of possible chain growth beyond C_2 for the latter route was attributed to the failure of the metal component to contribute to this support-catalysed step. Should such a process occur on the zeolite surface here, then the metal component must play some part since the rate of

formation and surface concentrations of the methyl formate intermediate are equivalent at any time on both zeolite and PdCu/zeolite (Fig. 5) but the formation of acetate species for PdCu/KL was always greater. This could indicate that two routes to acetate formation (10) are responsible for these differences. In fact when PdCu(0.5)/KL was reduced at 773 K, as opposed to 623 K in this study, bands were not detected at either ca 1710 or 1453 cm^{-1} (45), indicating the absence of methyl formate, although the band at 1567 cm^{-1}, indicative of the presence of acetate, was detected. This could be interpreted in terms of a more rapid isomerisation of methyl formate on the modified catalyst surface, with the intermediate concentration falling below the levels of detection. However, the strongest evidence against the latter route of carboxylic acid formation was that, in contrast to results reported for rare earth oxides (10), acetate species could not be generated by methyl formate adsorption on KL (Fig. 8). Acetate species may be assumed to form from acetyl species generated on the metal component of the catalyst followed by transfer to the zeolite surface in the same manner as indicated for formate species. The absence of the isomerisation route may be linked to the absence of a suitable Lewis acid site to assist in the migration of the carbenium ion (46), although sites of this nature are clearly identified by pyridine adsorption.

The Relationship between Detected Adsorbed Species, Reaction Products, and Hydrocarbon Formation

Although methyl formate is detected in significant quantities in contact with the catalyst within the infrared cell, methyl formate is apparently not eluted from the catalyst bed in the reactor and does not contribute to the oxygenate selectivity given in Table 1. TPD experiments show that above 473 K methyl formate is at least partially decomposed on the zeolite surface, giving the original syngas mixture. The absence of methyl formate in the reactor outlet contrasts with the behaviour of Pd/SiO_2 (12) and other copper-based catalysts, particularly alkali–metal promoted systems (39). DME was not detected as a reaction product (Table 1) nor was it observed in the IR cell. For palladium catalysts this may be attributed in part to the choice of KL as a support since palladium in the presence of a basic support shows high selectivity to methanol and low DME selectivity while DME formation is enhanced for acidic supports (47, 48). The absence of DME may be attributed, in part, to the absence of this support induced effect on the metal component (47). However, the detection of adsorbed acetate (Figs. 3, 4) may be significant as ether formation from methanol over zeolite catalysts is affected by the presence of acetic acid which poisons the basic sites in the zeolite surface which are required for stabilisation of the precursor in the formation of the carbocation intermediate (3, 6, 49). Of most importance is the failure to generate zeolite-bound methoxy species from the adsorption of methanol (Fig. 6) as there is considerable evidence which favors the intermediacy of these species in ether formation (3). Hutchings *et al.* (4) consider the methoxy species to be the common intermediate in the formation of methane and ethane as well as DME. This direct formation of the first C–C bond from methoxy groups, rather than via a DME intermediate, is supported in other reports (6, 28).

As neither surface methoxy nor DME have been detected for the KL-based catalysts, the formation of hydrocarbons via either of these intermediates must be ruled out. The progressive loss of threefold hollow sites on the Pd-enriched surfaces of these catalysts under the same reaction conditions has been reported (15) and it was suggested that this and the increased density of unoccupied states detected by XAS experiments may be attributed to the formation of carbonaceous surface species. However, while CO dissociation may be acceptable for Pd (48) and Pd-containing samples, similar observations in the XANES spectra of Cu/KL (15) and similar selectivities to methane and other hydrocarbons for the Pd and Pd-free catalysts (Table 1) indicate that the effects observed are probably not the result of CO dissociation and that this does not provide the principle route to hydrocarbon formation. Additionally, TPD experiments in H_2 following CO adsorption at 523 K failed to detect hydrogenation products which would be indicative of CO dissociation.

The adsorption of alcohols on NaZSM-5 may generate olefins via an intermediate containing a carbonyl group giving an IR band at 1710 cm^{-1} (6). In the case of butanols, oligomerisation led to the formation of long chain alkyl groups which remained attached to the zeolite surface (50, 51) or were transformed into alkenes (6). Similarly, here the presence of long chain alkyl groups giving a predominance of methylene groups would be consistent with the detection of the most intense band in the CH stretching region at 2933 cm^{-1} (Fig. 3) due to the CH stretching mode of CH_2 groups (17, 50, 51) which proved resistant to evacuation at 573 K (Fig. 3f). It is unlikely that the carbonyl-containing methyl formate detected here plays a role similar to the unidentified carbonyl detected for 2-propanol in the conversion to alkenes (6), as only decomposition products were evolved during the TPD experiments using methyl formate and no alkyl chains were detected by IR following heat treatment at 573 K in the presence of methyl formate or following room-temperature evacuation. Following chain termination, the alkyl chains are partially hydrogenated over the metallic function. In agreement with previous reports (52), Pd–Cu alloys exhibit enhanced hydrogenation activities relative to their monometallic components.

CONCLUSIONS

Pd, Cu, and PdCu loaded KL zeolites are active in the formation of methanol from synthesis gas. A synergetic

effect between copper and palladium on methanol production is observed in Pd-rich samples and attributed to an electronic effect of copper on surface palladium centres. Formate species at potassium sites in the zeolite react with methanol to produce methyl formate but the latter does not play any role in the formation of surface acetate and is not a precursor to hydrocarbon formation. Hydrogenation of alkenes is more favorable over bimetallic than monometallic samples.

ACKNOWLEDGMENTS

We thank the Royal Society (London) for a University Research Fellowship (JAA), the CSIC (Spain) for a Postdoctoral Contract (M.F.-G.), Professor J. L. G. Fierro (Madrid) for the use of the high pressure reactor and TPD apparatus, Professor C. H. Rochester (Dundee) for the use of the IR spectrometer, Professor G. L. Haller (Yale) for helpful discussions regarding KL zeolites, and Professor M. Bowker (Reading) for discussions regarding CO dissociation on PdCu crystal surfaces.

REFERENCES

1. Fujimoto, K., Kudo, Y., and Tominaga, H., *J. Catal.* **87**, 136 (1984).
2. Chang, C. D., Lang, W. H., and Silvestri, A. J., *J. Catal.* **56**, 268 (1979).
3. Chang, C. D., *Catal. Rev.-Sci. Eng.* **25**, 1 (1983).
4. Hutchings, G. J., Hunter, R., Johnston, P., and Jansen van Rensburg, L., *J. Catal.* **142**, 602 (1991).
5. Haldor Topsoe, U.S. Patent 4,536,458 (1993).
6. Bezoukhanova, C. P., and Kalachev, Y. A., *Catal. Rev.-Sci. Eng.* **51**, 125 (1994).
7. Matsumura, Y., Hashimoto, K., and Yoshida, S., *J.C.S. Chem. Commun.* 1447 (1984).
8. Matsumura, Y., Hashimoto, K., and Yoshida, S., *J. Catal.* **100**, 392 (1986).
9. Tempesti, E., Kiennemann, A., Rapagna, S., Mazzoccchia, C., and Giuffre, L., *Chem. Ind.* 548 (1991).
10. Chateau, L., Hindermann, J. P., Kiennemann, A., and Tempesti, E., *J. Molec. Catal.* **107**, 367 (1996).
11. Davies, P., Snowdon, F. F., Bridger, G. W., Hughes, D. O., and Young, P. W., U.K. Patent 1,010,871.
12. Poutsma, M. L., Elek, L. F., Ibarbia, P. A., Risch, A. P., and Rabo, J. A., *J. Catal.* **52**, 157 (1978).
13. Ponec, V., *Surf. Sci.* **272**, 111 (1992).
14. Fernández-García, M., Anderson, J. A., and Haller, G. L., *J. Phys. Chem.* **100**, 16247 (1996).
15. Anderson, J. A., Fernández-García, M., and Haller, G. L., *J. Catal.* **164**, 477 (1996).
16. Leon y Leon, C. A., and Vannice, M. A., *Appl. Catal.* **69**, 305 (1991).
17. Anderson, J. A., McQuire, M. W., Rochester, C. H., and Sweeney, T., *Catal. Today* **9**, 23 (1991).
18. Anderson, J. A., and Khader, M. M., *J. Molec. Catal.* **105**, 175 (1996).
19. Morrow, B. A., *J.C.S. Faraday Trans. 1* **70**, 1528 (1974).
20. Ward, J. W., *in* "Zeolite Chemistry and Catalysis" (J. A. Rabo, Ed.), ACS monograph, Vol. 118. Am. Chem. Soc., Washington, DC, 1976.
21. Aronson, M. T., Gorte, R. J., and Farneth, W. E., *J. Catal.* **105**, 455 (1987).
22. Forester, T. R., and Howe, R. F., *J. Am. Chem. Soc.* **109**, 5076 (1987).
23. Menacherry, P. V., and Haller, G. L., *Catal. Lett.* **44**, 135 (1997).
24. Newell, P. A., and Rees, L. V. C., *Zeolites* **3**, 22, 28 (1983).
25. Highfield, J. G., and Moffat, J. B., *J. Catal.* **98**, 245 (1986).
26. Blaszkowski, S. R., and van Santen, R. A., *J. Phys. Chem.* **101**, 2292 (1997).
27. van Santen, R. A., and Kramer, G. J., *Chem. Rev.* **95**, 637 (1995).
28. Kubelková, L., Nováková, J., and Nedomová, K., *J. Catal.* **124**, 441 (1990).
29. Millar, G. J., Rochester, C. H., and Waugh, K. C., *J. Catal.* **142**, 263 (1993).
30. Raskó, J., Bontovics, J., and Solymosi, F., *J. Catal.* **146**, 22 (1994).
31. Hughes, T. R., Buss, W. C., Tamm, P. W., and Jacobson, R. L., *in* "New Developments in Zeolite Science and Technology" (Y. Murakami, A. Iijima, and J. W. Ward, Eds.), p. 725. Elsevier, Amsterdam, 1986.
32. Ison, A., and Gorte, R., *J. Catal.* **89**, 150 (1984).
33. Hertl, W., and Cuenca, A. M., *J. Phys. Chem.* **77**, 1120 (1973).
34. Kagel, R. O., and Greenler, R. G., *J. Chem. Phys.* **49**, 1638 (1968).
35. He, M.-Y., and Ekerdt, J. G., *J. Catal.* **87**, 381 (1984).
36. Gopal, P. G., Schneider, R. L., and Watters, K. L., *J. Catal.* **105**, 366 (1987).
37. Deluzarche, A., Hindermann, J.-P., Kiennemann, A., and Kieffer, R., *J. Molec. Catal.* **31**, 225 (1985).
38. Millar, G. J., Rochester, C. H., and Waugh, K. C., *J.C.S. Faraday Trans.* **88**, 3497 (1992).
39. Millar, G. J., Rochester, C. H., and Waugh, K. C., *J.C.S. Faraday Trans.* **87**, 2785 (1991).
40. Ray, D. J. M. (BP Chemicals Ltd.), *Eur. Pat. Appl.* EP 60,695 (1982).
41. Amenomiya, Y., *J. Catal.* **57**, 64 (1979).
42. Tagawa, T., Pleizer, G., and Amenomiya, Y., *Appl. Catal.* **18**, 285 (1985).
43. Millar, G. J., Rochester, C. H., and Waugh, K. C., *J.C.S. Faraday Trans.* **87**, 1467 (1991).
44. Fernández-García, M., Conesa, J. C., Ricart, J. M., Clotet, A., López, N., and Illas, F., *J. Phys. Chem. B* **102**, 141 (1998).
45. Anderson, J. A., unpublished.
46. Kositsyna, N. Y., and Moiseev, I. I., *Kinet. Catal.* **32**, 985 (1991).
47. Berlowitx, P. J., and Goodman, D. W., *J. Catal.* **108**, 364 (1987).
48. Xu, M., Goodman, D. W., and Bhattacharyya, A., *Appl. Catal.* **149**, 303 (1997).
49. Santacesaria, E., Gelosa, D., Giorgi, E., and Carra, S., *J. Catal.* **90**, 1 (1984).
50. Williams, C., Makarova, M. A., Malysheva, L. V., Paukshtis, E. A., Zamaraev, K. I., and Thomas, J. M., *J.C.S. Faraday Trans.* **86**, 3473 (1990).
51. Williams, C., Makarova, M. A., Malysheva, L. V., Paukshtis, E. A., Talsi, E. P., Thomas, J. M., and Zamaraev, K. I., *J. Catal.* **127**, 377 (1991).
52. Lianos, L., Debauge, Y., Massadier, J., Jugnet, Y., and Bertolini, J. C., *Catal. Lett.* **44**, 211 (1997).